

东昆仑浪麦滩地区 A 型花岗岩年代学、地球化学特征及其地质意义

李金超¹⁾, 国显正²⁾, 孔会磊¹⁾, 姚学钢¹⁾, 贾群子¹⁾

1) 中国地质调查局西安地质调查中心, 自然资源部岩浆作用成矿与找矿重点实验室, 陕西西安, 710054;

2) 合肥工业大学资源与环境工程学院, 安徽合肥, 230009

内容提要:东昆仑造山带出露大面积的花岗岩, 是研究岩浆活动的天然实验室, 晚三叠世 A 型花岗岩为该区构造演化提供了新的约束。本文通过对东昆仑浪麦滩地区出露的正长花岗岩开展岩相学、锆石 U-Pb 定年、Hf 同位素及地球化学研究, 以期限定其形成时代, 探讨岩石成因, 并为区域构造岩浆演化提供依据。正长花岗岩由正长石、条纹长石、斜长石、石英和少量黑云母等矿物组成。LA-ICP-MS 锆石 U-Pb 年龄为 231.5 ± 1.7 Ma, 形成于晚三叠世。岩石地球化学具有高硅富铝特征, SiO_2 含量为 72.36%~74.58%, Al_2O_3 含量为 12.76%~12.89%, 相对富钾贫钠, K_2O 、 Na_2O 含量分别为 4.43%~4.96%、4.0%~4.25%, 低 MgO、 TiO_2 , 富集 Rb、K 等大离子亲石元素, 强烈亏损 Ba、Nb、Ta、P、Ti 等高场强元素, 具有明显的负铕异常 ($\delta\text{Eu}=0.040\sim0.08$), 表明为 A 型花岗岩。 $\text{Mg}^\#$ 介于 0.40~0.43 之间, $\epsilon_{\text{Hf}}(t)$ 值介于 +2.05~+7.53 之间, 二阶段 Hf 模式年龄 $T_{\text{DM}2}$ 为 782~1132 Ma, 指示源区有幔源岩浆物质的参与。综合分析表明, 在后碰撞伸展背景下由于幔源岩浆底侵, 新生地壳部分熔融并混入幔源物质, 最终形成浪麦滩地区 A 型花岗岩。

关键词:正长花岗岩; 锆石 U-Pb 定年; 地球化学; Lu-Hf 同位素; 东昆仑

A 型花岗岩, 指的是一种具有非造山、无水以及碱性等特征的一种特殊花岗岩 (Loiselle, 1979); 在矿物学上, 暗色矿物组成主要为富含铁的含水镁铁质矿物 (Loiselle, 1979; King et al., 1997); 地球化学方面, 通常具有高 TFeO/MgO、Ga/Al 比值, 富碱, 具有高含量 $\text{K}_2\text{O}+\text{Na}_2\text{O}$ 等特征, 富集高场强元素 (Zr、Nb 等) 和三价稀土元素 (REE^{+3}) (Eby, 1990; Anderson et al., 2003; Lei et al., 2013; Huang et al., 2019)。通常情况下, A 型花岗岩既可以形成于板内的伸展环境, 也可以形成于碰撞后板块边缘的伸展环境 (Whalen et al., 1987; Eby, 1990; Bonin, 2007)。尽管 A 型花岗岩类仅占花岗岩类的一小部分, 但这类花岗岩的研究有助于加深对大陆岩石圈后碰撞或板内伸展岩浆作用的理解 (Eby and Nelson, 1992; Mushkin et al., 2003), 具

有重要的地球动力学意义, 备受国内外学者的关注。因此, 通过对 A 型花岗岩的研究, 可以探讨其产出的动力学背景, 进而限定区域构造演化, 具有十分重要的意义。

目前东昆仑造山带报道的 A 型花岗岩主要分布在东昆仑中段和祁漫塔格地区, 时代主要为晚志留世到泥盆纪以及晚三叠世, 如 Li Guochen et al. (2012) 在白干湖地区获得 A 型花岗岩年龄 422 ± 3 Ma、 421 ± 3.7 Ma; Wang Guan et al. (2013) 获得夏日哈木 A 型正长花岗岩年龄 391 ± 1 Ma; Yan Wei et al. (2016) 报道了猴头沟二长花岗岩年龄 419 ± 1.9 Ma, 并认为属于 A 型花岗岩; Liu Lei et al. (2019) 在群力地区获得正长花岗岩年龄 376 ± 2 Ma; Chen et al. (2020) 在五龙沟西和沟里地区分别获得 A 型花岗岩年龄 418 ± 3 Ma 和 403 ± 2 Ma, 并

注: 本文为第二次青藏高原综合科学考察研究项目 (编号 2019QZKK0801)、中国地质调查局项目 (编号 DD20190143, DD20160013) 资助的成果。

收稿日期: 2020-10-28; 改回日期: 2020-12-14; 网络发表日期: 2020-12-21; 责任编辑: 吴才来; 责任编辑: 周健。

作者简介: 李金超, 男, 1976 年生。高级工程师, 主要从事区域成矿及成矿规律等方面的研究工作。E-mail: lijinchao0313@163.com。通讯作者: 国显正, 男, 1990 年生。博士, 从事岩石学、矿床学与成矿规律研究。E-mail: cuggxz@126.com。

引用本文: 李金超, 国显正, 孔会磊, 姚学钢, 贾群子. 2021. 东昆仑浪麦滩地区 A 型花岗岩年代学、地球化学特征及其地质意义. 地质学报, 95(5): 1508~1522, doi: 10.19762/j.cnki.dizhixuebao.2021115.
Li Jinchao, Guo Xianzheng, Kong Huilei, Yao Xuegang, Jia Qunzi. 2021. Geochronology, geochemical characteristics and geological significance of A-type granite from the Langmaitanarea, East Kunlun. Acta Geologica Sinica, 95(5): 1508~1522.

详细总结了东昆仑原特提斯 A 型花岗岩特征;相比原特提斯,东昆仑古特提斯 A 型花岗岩研究较少,主要出露在祁漫塔格地区(Chen Danling et al., 2001);Gao Yongbao et al. (2014)在野马泉获得 213 ± 1 Ma 的正长花岗岩,认为形成于后碰撞阶段;Qian Bing et al. (2015)在于沟子获得钾长花岗岩年龄 210 ± 0.6 Ma,该 A 型花岗岩形成于后造山阶段,Zhang Mingyu et al. (2018)对肯德可克正长花岗岩进行研究,获得锆石 U-Pb 年龄为 217.9 ± 1.7 Ma,形成于造山后伸展环境。由此可见关于东昆仑古特提斯碰撞—后碰撞构造阶段的结束,以及 A 型花岗岩形成的构造背景尚不明确,同时在东昆仑其他地区 A 型花岗岩鲜有报道,制约了对区内岩石形成环境的认识。项目组在东昆仑东段浪麦滩地区发现出露有晚三叠世 A 型花岗岩,本文对其开展锆石 U-Pb 年代学、岩石地球化学和同位素地球化学研

究,探讨岩石成因及成岩构造背景,以期东昆仑古特提斯岩浆作用和构造演化提供参考和依据。

1 地质概况

东昆仑造山带位于青藏高原北缘,大地构造位置隶属中央造山系西段(Xu Zhiqin et al., 2006; Mo Xuanyue et al., 2007),北以柴达木盆地南缘为界,南以昆南断裂和昆仑山口—甘德断裂为界与巴颜喀拉造山带相邻,东被温泉断裂截切与西秦岭造山带相邻,西被阿尔金断裂截切与西昆仑造山带相邻(图 1a、b)。该造山带出露大面积的花岗岩,是我国可与冈底斯相媲美的一条重要的构造岩浆活动带(Mo Xuanyue et al., 2007),主要出露中酸性岩石,如闪长岩、花岗闪长岩、二长花岗岩、正长花岗岩等(Chen Guochao et al., 2019; Guo Xianzheng et al., 2019b),同时零星出露镁铁超镁铁岩,少量伴

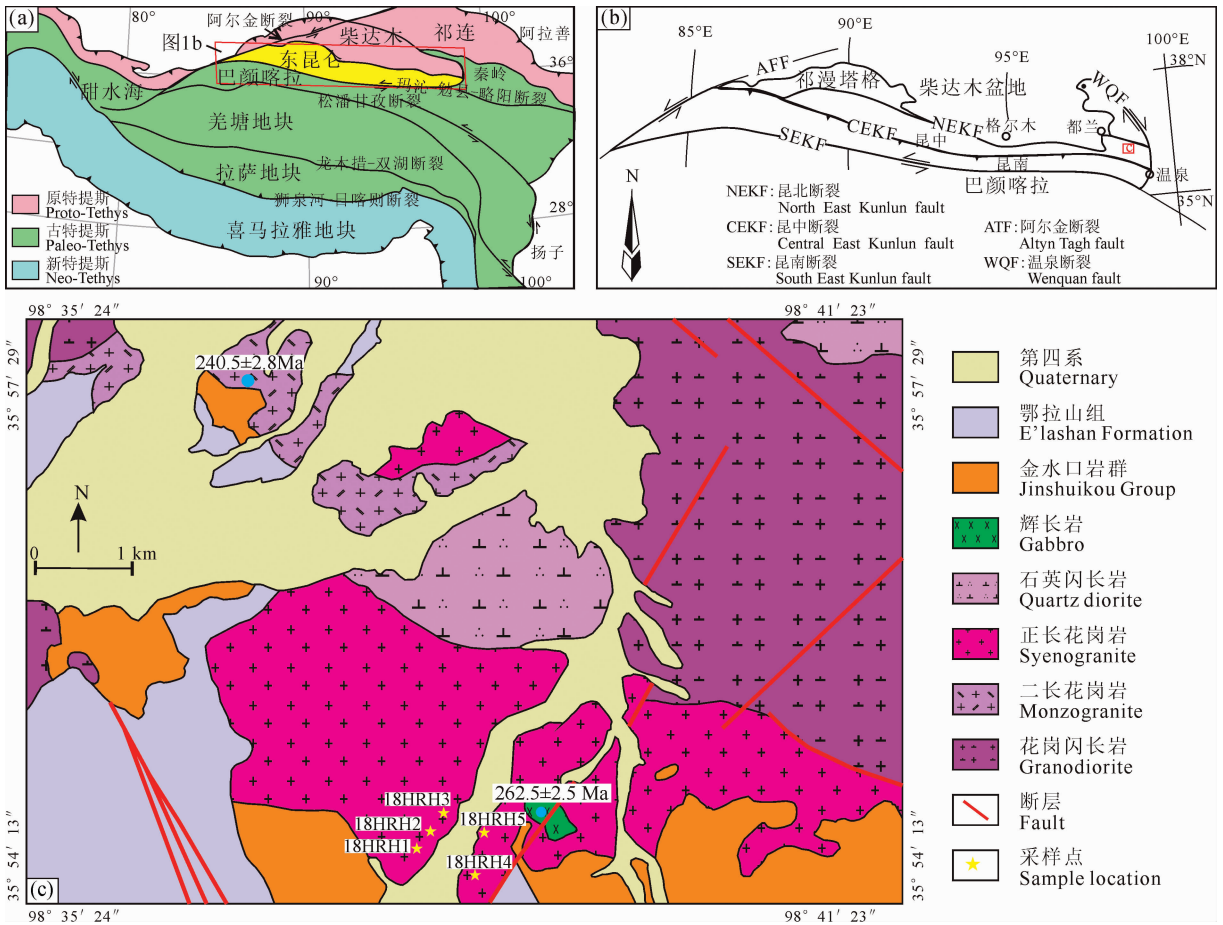


图 1 东昆仑浪麦滩地区地质简图

Fig. 1 The sketch geological map of the Langmaitan, East Kunlun

(a)—青藏高原构造简图;(b)—东昆仑构造简图(据 Xia et al., 2015);(c)—浪麦滩地区地质简图

(a)—Simplified tectonic map of Tibetan Plateau; (b)—simplified tectonic map of East Kunlun (after Xia et al., 2015);

(c)—sketch geological map of the Langmaitan area

有镍多金属矿化(Zhang Zhaowei et al., 2015; Song et al., 2016; Liu et al., 2018)。该造山带广泛出露的岩浆岩,形成时间跨度大,主要集中在古生代和中生代两个时期(Liu Bin et al., 2012; Ma Changqian et al., 2015; Shao et al., 2017; Guo Xianzheng et al., 2018b),分别记录了东昆仑造山带原特提斯和古特提斯俯冲—碰撞—增生造山完整演化史(Yu et al., 2017; Dong et al., 2018; Xin et al., 2019)。

浪麦滩地区位于青海省都兰县境内,大地构造位置处于东昆仑造山带东段,夹持于昆南构造混杂岩带与昆北(祁漫塔格)构造带之间(Dong et al., 2018; Guo Xianzheng et al., 2018a; Chen Guochao et al., 2019)。由于受区域构造控制,浪麦滩地区地层及岩体展布方向主要呈北西向,近东西向。浪麦滩地区出露岩浆岩主要为花岗闪长岩、二长花岗岩、石英闪长岩等,少量辉长岩等(图 1c)。本文研究的正长花岗岩位于浪麦滩南部地区,南侧为金水口岩群,二者呈侵入接触关系,接触界线截然,未见矽卡岩化、角岩化等现象;东北侧为花岗闪长岩,二者呈断层接触关系;北侧为石英闪长岩,二者呈突变

接触关系;正长花岗岩西侧为鄂拉山组火山岩,二者呈角度不整合接触关系:鄂拉山组火山岩覆盖在正长花岗岩上,Guo Xianzheng et al. (2019a)在邻区那更康切尔鄂拉山组中获得流纹岩锆石 U-Pb 年龄 217.4 ± 3.1 Ma,表明该套火山岩在晚三叠世已经形成。西北侧主要出露二长花岗岩,Yao Xuegang et al. (2018)获得二长花岗岩锆石 U-Pb 年龄 240.5 ± 2.8 Ma。该区辉长岩形成于晚二叠世,Kong Huilei et al. (2017)测得辉长岩锆石年龄 262.5 ± 2.5 Ma。

2 样品和分析方法

本次研究选取 18HRH3 作为锆石 U-Pb 测年和 Lu-Hf 同位素分析样品,采样坐标 $N35^{\circ}54'33''$, $E98^{\circ}38'08''$,同时采集 5 件新鲜岩石样品进行地球化学分析(图 1c)。正长花岗岩样品新鲜面为肉红色,中粗粒花岗结构,块状构造(图 2a、b),主要由正长石、条纹长石、斜长石、石英、黑云母等矿物组成(图 2c、d);碱性长石含量约 55%~60%,粒径 3~8 mm,手标本中部分粒径可见卡式双晶;斜长石含量

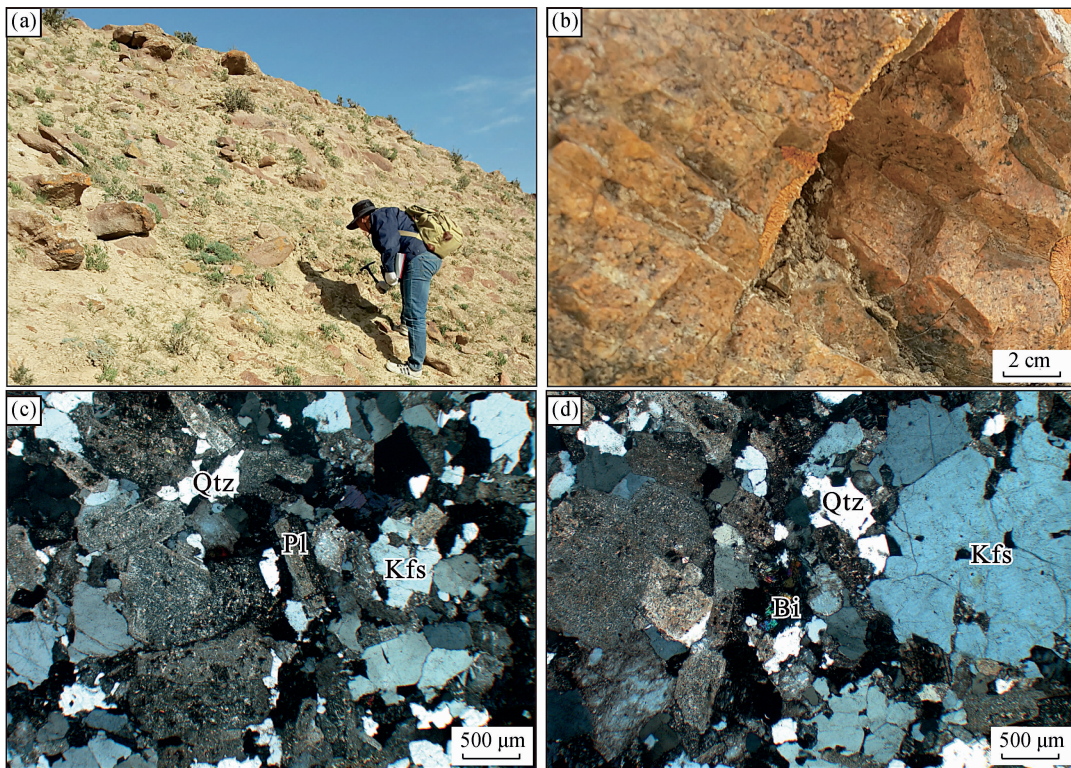


图 2 浪麦滩正长花岗岩手标本和镜下显微照片

Fig. 2 Field photograph and microphotographs of Langmaitan syenogranite

(a)—正长花岗岩野外露头;(b)—正长花岗岩手标本;(c、d)—镜下特征(正交偏光);Pl—斜长石;Kfs—钾长石;Qtz—石英;Bi—黑云母
(a)—Outcrop for the syenogranite; (b)—sample for the syenogranite; (c, d)—photomicrographs for the syenogranite (crossed polarized light); Pl—plagioclase; Kfs—K-feldspar; Qtz—quartz; Bi—biotite

15%~20%,板柱状,粒径 3~6 mm 不等;石英约 20%~25%,自形粒状,黑云母约 5%,多为鳞片状;副矿物有磷灰石、榍石、锆石等。碱性长石主要为正长石和条纹长石,晶体呈粒状或不规则粒状,与石英或斜长石矿物接触界线平直;斜长石多发育绢云母化,黑云母多被绿泥石交代(图 2d)。

岩石主微量元素测试在中国地质调查局西安地质调查中心自然资源部岩浆作用成矿与找矿重点实验室完成,测试结果见表 1。主量元素采用 X 射线荧光光谱(XRF)进行分析,分析精度优于 1%;其中 FeO 含量通过湿化学方法测定;稀土和微量元素采用 SX50 型电感耦合等离子质谱仪(ICP-MS)分析,仪器采用美国热电(Thermochemical X7)ICPMS,分析精度优于 5%。

正长花岗岩样品锆石分选、制靶和阴极发光图像分析均在北京前寒武科技有限公司完成。样品先经过清洁,然后经碎样机粉碎至 80 目,再经过淘洗、重磁选,之后在双目镜下进行观察和随机挑选,最后将挑选好的无裂隙、干净透明、自形程度较好的锆石颗粒粘帖到双面胶上,用环氧树脂固定制成 2.5 cm 的圆形靶进行透射光、反射光及阴极发光图像分析。

正长花岗岩锆石 U-Pb 定年和微量元素分析, Hf 同位素分析在中国地质调查局西安地质调查中心自然资源部岩浆作用成矿与找矿重点实验室完成。锆石 U-Pb 测年采用 193 nm ArF 准分子(excimer)激光器的 Geo Las200M 剥蚀系统,剥蚀物质以 He 作为载气,ICP-MS 为 Agilent7700,激光束斑直径 24 μm 。以国际标准锆石 91500 作为外标准矿物,元素含量采用 NIST SRM610 作为外标,²⁹Si 作为内标元素(Yuan et al., 2008),仪器详细参数及操作方法参考 Li Yanguang et al. (2015);数据处理应用 Glitter (ver4.0, Macquarie University)程序,年龄计算及谐和图的绘制采用 Isoplot 软件。锆石 Hf 同位素分析仪器采用 193 nm 激光的 Neptune 多接收电感耦合等离子质谱仪进行分析,根据已测年单点结果和锆石颗粒大小,选择相同或叠加 1/3 位置进行 Hf 同位素分析,激光束斑直径 32 μm ,频率 10 Hz,采用国际标准锆石 91500 进行监控和样品外部校正。计算 $\epsilon_{\text{Hf}}(t)$ 值时, Lu 衰变常数采用 $1.867 \times 10^{-11}/\text{a}$ (Söderlund et al., 2004),球粒陨石的 ¹⁷⁶Hf/¹⁷⁷Hf 值为 0.282785, ¹⁷⁶Lu/¹⁷⁷Hf 值为 0.0336 (Bouvier et al., 2008)。Hf 亏损地幔模式年龄的计算采用现今的亏损地幔 ¹⁷⁶Hf/¹⁷⁷Hf 值为 0.28325 和 ¹⁷⁶Lu/¹⁷⁷Hf 值为 0.0384 (Griffin et al., 2000)。

表 1 浪麦滩正长花岗岩主量元素(%)和微量元素($\times 10^{-6}$)含量

Table 1 Contents of major elements (%) and trace elements ($\times 10^{-6}$) of Langmaitan syenogranite

送样号	18HR-H1	18HR-H2	18HR-H3	18HR-H4	18HR-H5
SiO ₂	72.82	74.17	73.66	73.83	74.58
TiO ₂	0.20	0.18	0.18	0.18	0.18
Al ₂ O ₃	12.81	12.76	12.83	12.89	12.84
Fe ₂ O ₃	1.31	1.70	1.64	1.70	1.55
FeO	1.19	0.58	0.69	0.65	0.60
MnO	0.06	0.05	0.07	0.05	0.05
MgO	0.88	0.88	0.86	0.81	0.86
CaO	0.97	0.44	0.37	0.50	0.30
Na ₂ O	4.00	4.09	4.23	4.25	4.23
K ₂ O	4.43	4.96	4.90	4.83	4.90
P ₂ O ₅	0.02	0.02	0.02	0.02	0.02
LOI	1.26	0.91	1.27	0.90	0.63
Total	99.95	100.74	100.72	100.61	100.73
Mg#	0.40	0.43	0.42	0.40	0.43
A/CNK	0.97	0.99	0.99	0.98	1.00
A/NK	1.12	1.05	1.05	1.05	1.05
Cs	3.34	11.50	3.64	2.95	3.58
Rb	158.00	189.00	185.00	178.00	183.00
Ba	69.80	67.40	52.50	54.40	65.60
Sr	41.20	28.00	23.00	28.80	27.30
Th	22.20	20.70	22.10	24.40	24.00
U	3.43	2.76	4.09	4.02	4.17
Nb	34.60	36.00	39.20	39.00	40.90
Ta	2.56	2.31	2.76	2.86	2.91
Zr	446.00	511.00	539.00	465.00	522.00
Hf	12.10	12.00	12.60	12.30	13.10
Co	4.79	0.54	0.30	0.45	0.40
Ni	17.80	1.17	0.91	1.11	1.38
Cr	47.60	3.81	3.68	5.08	4.90
V	10.60	2.82	1.53	2.75	2.06
Sc	10.50	6.99	7.32	6.70	8.21
Ga	24.30	22.10	25.40	23.60	24.70
Cu	6.28	2.81	2.60	2.48	2.78
Pb	31.50	32.50	33.70	34.30	41.00
Zn	83.40	85.60	70.10	67.70	64.00
Sn	3.62	4.23	4.07	4.00	4.08
La	65.30	73.00	73.60	77.40	76.40
Ce	127.00	136.00	135.00	145.00	151.00
Pr	14.80	15.90	15.60	16.40	16.40
Nd	51.00	56.70	57.00	57.60	58.30
Sm	9.70	10.30	10.50	10.60	10.40
Eu	0.23	0.15	0.15	0.15	0.14
Gd	8.34	8.68	9.11	9.00	9.15
Tb	1.41	1.41	1.46	1.47	1.42
Dy	8.53	7.65	8.24	8.31	8.30
Ho	1.81	1.56	1.68	1.75	1.70
Er	5.00	4.51	4.75	5.05	4.98
Tm	0.78	0.66	0.72	0.74	0.74
Yb	4.96	4.33	4.81	4.89	4.98
Lu	0.79	0.68	0.76	0.79	0.77
Y	35.40	33.60	37.00	38.20	37.50
ΣREE	299.64	321.53	323.38	339.15	344.68
LREE	268.03	292.05	291.85	307.15	312.64
HREE	31.62	29.48	31.54	32.00	32.05
LREE/HREE	8.48	9.91	9.25	9.60	9.76
La _N /Yb _N	9.44	12.09	10.98	11.35	11.00
δEu	0.08	0.05	0.05	0.05	0.04
δCe	1.00	0.98	0.98	1.00	1.05

3 测试结果

3.1 主量元素特征

浪麦滩正长花岗岩具有高硅富铝特征, SiO_2 含量介于 72.36%~74.58% 之间, 平均 73.81%, Al_2O_3 含量介于 12.76%~12.89% 之间, 平均 12.83%; 相对富碱, 全碱含量 $\text{Na}_2\text{O} + \text{K}_2\text{O}$ 介于 8.43%~9.13% 之间, 富钾贫钠, K_2O 、 Na_2O 含量分别为 4.43%~4.96%、4.00%~4.25%。在 TAS 图解中(图 3a), 落入花岗岩区域; 在 SiO_2 -($\text{K}_2\text{O} + \text{Na}_2\text{O} - \text{CaO}$)图解中(图 3b), 为碱钙质系列; 在 SiO_2 - K_2O 图解中(图 3c)落入高钾钙碱性系列。铝饱和指数 A/CNK 较为集中, 比值介于 0.97~1.00 之间, 平均为 0.99。A/NK 介于 1.05~1.12 之间, 平均为 1.06。在 A/CNK-A/NK 图解中样品主要落

在准铝质区域(图 3d)。

3.2 微量元素特征

浪麦滩正长花岗岩稀土元素总量 ΣREE 介于 $299.64 \times 10^{-6} \sim 344.68 \times 10^{-6}$ 之间, 平均为 325.68×10^{-6} ; 相对富集轻稀土, 亏损重稀土, LREE/HREE 比值为 8.48~9.91, 平均为 9.40, La_N/Yb_N 介于 9.44~12.09 之间, 平均 10.97, 稀土元素配分曲线图中呈富 LREE 的右倾曲线(图 4a); 具有低的负铕异常值, δEu 值介于 0.04~0.08 之间, 表明源区有斜长石的残留或成岩过程中斜长石发生了较强的分离结晶作用。

正长花岗岩具有高 Rb ($158 \times 10^{-6} \sim 189 \times 10^{-6}$), 高 Zr ($446 \times 10^{-6} \sim 539 \times 10^{-6}$), Ce ($127 \times 10^{-6} \sim 151 \times 10^{-6}$), Ga ($22.1 \times 10^{-6} \sim 25.4 \times 10^{-6}$), 低 Sr ($23 \times 10^{-6} \sim 41.2 \times 10^{-6}$) 和 Nd ($51 \times$

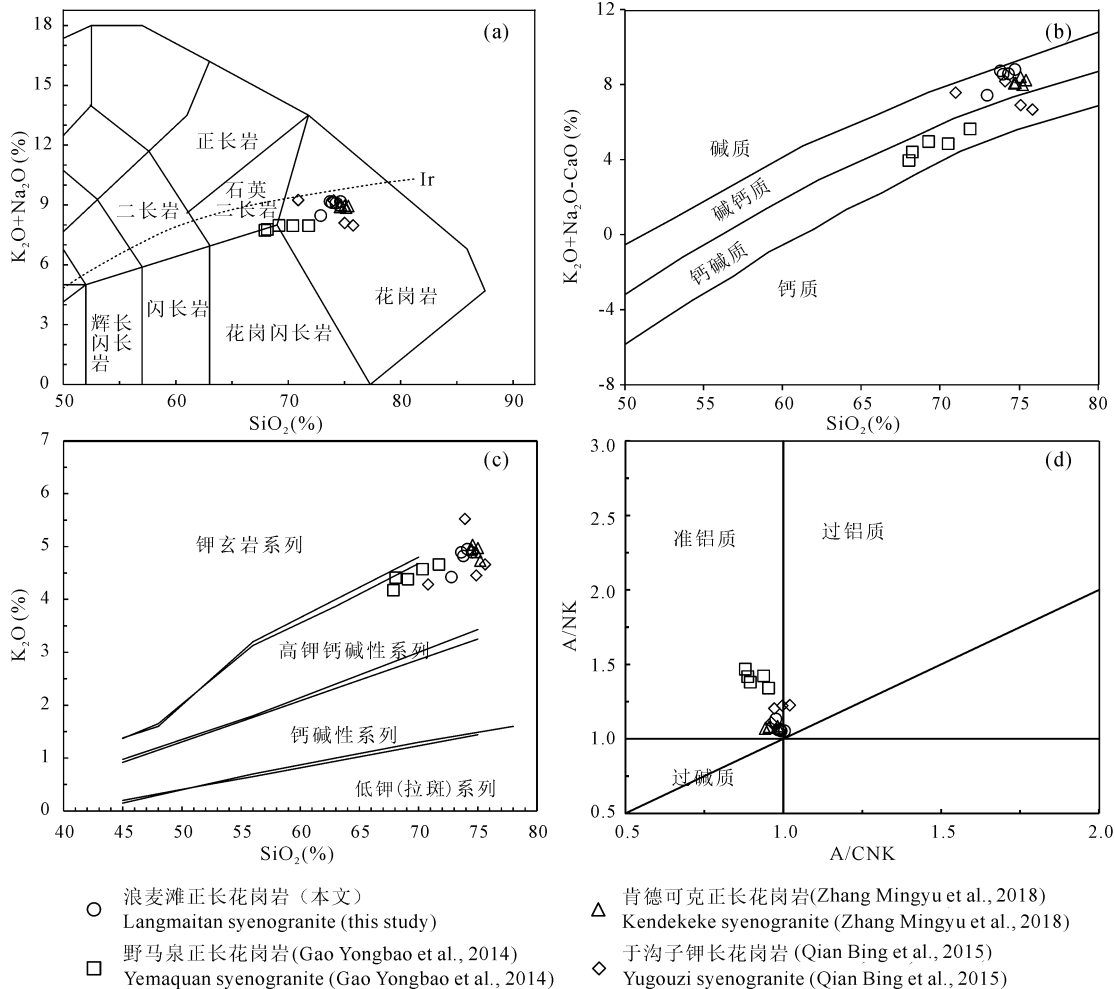


图3 浪麦滩正长花岗岩 TAS 图解(a)(底图据 Middlemost, 1994)、 SiO_2 -($\text{K}_2\text{O} + \text{Na}_2\text{O} - \text{CaO}$)图(b)(底图据 Peccerillo and Taylor, 1976)、 SiO_2 - K_2O 图解(c)(底图据 Frost, 2001)和 A/NK-A/CNK 图(d)(底图据 Maniar and Piccoli, 1989)

Fig. 3 TAS diagram (a) (after Middlemost, 1994), SiO_2 -($\text{K}_2\text{O} + \text{Na}_2\text{O} - \text{CaO}$) diagram (b) (after Peccerillo and Taylor, 1976), SiO_2 - K_2O diagram (c) (Frost, 2001) and A/NK-A/CNK diagram (d) (after Maniar and Piccoli, 1989) of Langmaitan syenogranite

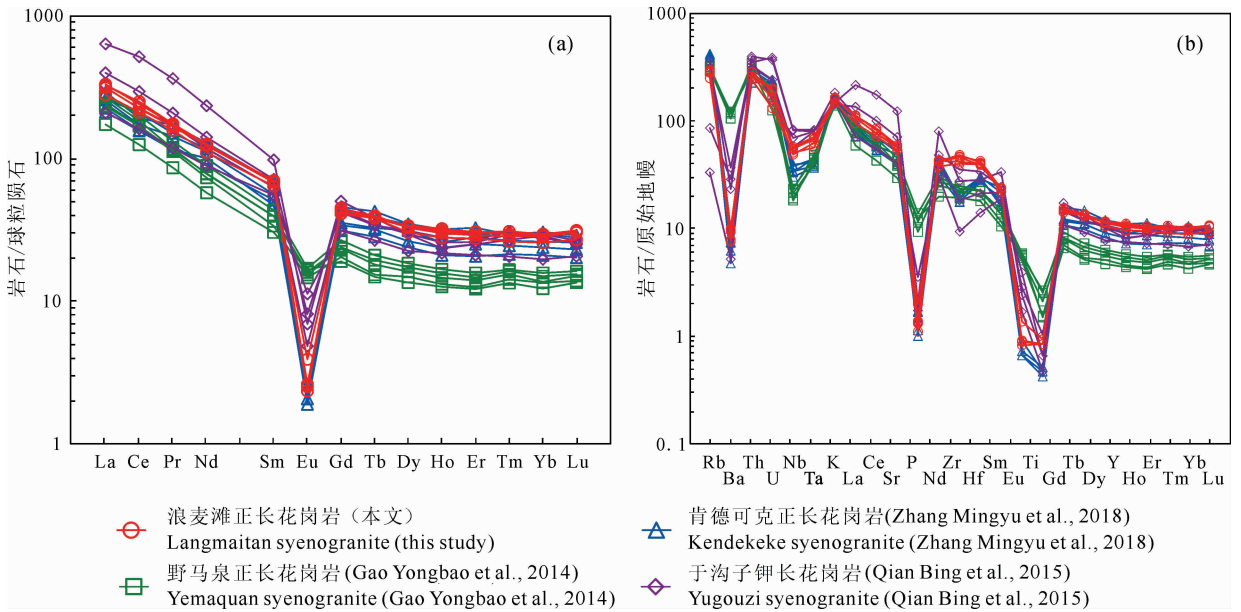


图 4 浪麦滩正长花岗岩的稀土元素球粒陨石标准化配分曲线图(a)和微量元素原始地幔标准化蛛网图(b)
(标准化数据据 Sun and McDonough,1989)

Fig. 4 Chondrite-normalized REE patterns (a) and Primitive mantle-normalized trace element patterns (b) for the Langmaitan syenogranite (normalized values after Sun and McDonough,1989)

$10^{-6} \sim 58.3 \times 10^{-6}$) 等特征。在微量元素蛛网图上(图 4b)岩石总体上富集 Rb、K 等大离子亲石元素,亏损 Ba、Nb、Ta、P、Ti 等高场强元素,暗示源区斜长石、金红石等矿物分离结晶。

3.3 锆石 U-Pb 定年

正长花岗岩锆石 U-Pb 分析测试结果见表 2。Cl 阴极发光图显示锆石内部结构特征(图 5),锆石形态呈长柱状,自形程度较好,粒径约 $50 \sim 150 \mu\text{m}$,长宽比在 $2:1 \sim 3:1$ 之间,可见明显的韵律振荡环带。锆石 Th 含量在 $154.84 \times 10^{-6} \sim 319.97 \times 10^{-6}$

之间,U 含量在 $239.94 \times 10^{-6} \sim 51.84 \times 10^{-6}$ 之间,Th/U 值为 $0.41 \sim 0.87$;锆石微量元素测试结果见表 3,稀土配分模式图显示出重稀土富集、相对亏损轻稀土元素特征,显示典型的岩浆锆石成因特征(Hoskin and Schaltegger,2003)。本次共测试 24 个点,获得 23 个有效测点,数据 $^{206}\text{Pb}/^{238}\text{U}$ 模式年龄介于 $228.0 \sim 234.8 \text{ Ma}$ 之间。在 $^{206}\text{Pb}/^{238}\text{U}$ - $^{207}\text{Pb}/^{235}\text{U}$ 年龄谱和曲线图中,测点数据均投影在谐和线上,其 $^{206}\text{Pb}/^{238}\text{U}$ 加权平均年龄为 $231.5 \pm 1.7 \text{ Ma}$ (MSWD=0.19)(图 6)。

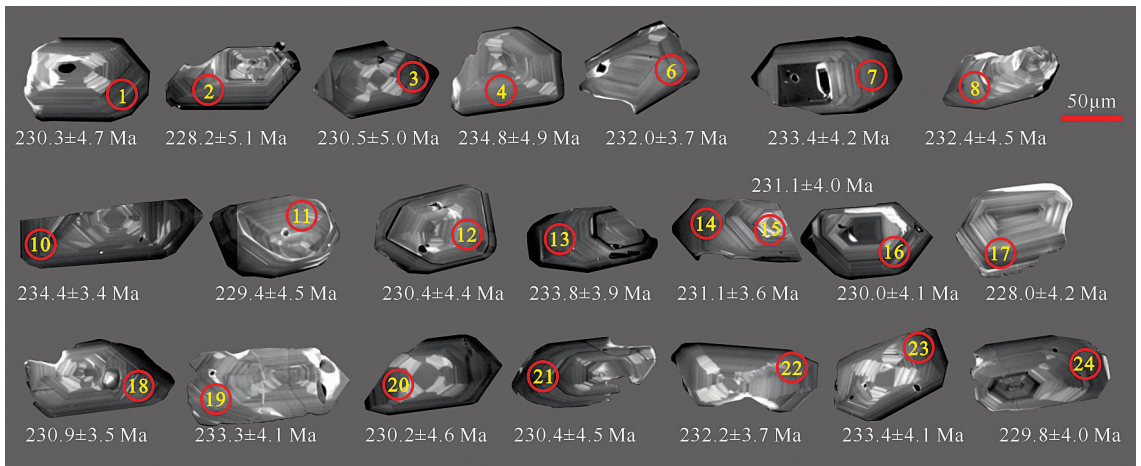


图 5 浪麦滩正长花岗岩锆石阴极发光图像及年龄(圈内数字代表分析点,圈外数字代表 $^{206}\text{Pb}/^{238}\text{U}$ 表面年龄)

Fig. 5 CL images of zircons and age from Langmaitan syenogranite (the numbers in the circle represent the analysis points, the numbers outside the circle represent the $^{206}\text{Pb}/^{238}\text{U}$ age)

表 2 浪麦滩正长花岗岩锆石 LA-ICP-MS 测年结果

Table 2 LA-ICP-MS U-Pb isotopic data of zircon from Langmaitan syenogranite

测试点	含量($\times 10^{-6}$)		Th/U	同位素比值						年龄(Ma)					
	Th	U		$^{207}\text{Pb}/^{206}\text{Pb}$	$\pm 1\sigma$	$^{207}\text{Pb}/^{235}\text{U}$	$\pm 1\sigma$	$^{206}\text{Pb}/^{238}\text{U}$	$\pm 1\sigma$	$^{207}\text{Pb}/^{206}\text{Pb}$	$\pm 1\sigma$	$^{206}\text{Pb}/^{238}\text{U}$	$\pm 1\sigma$	$^{207}\text{Pb}/^{235}\text{U}$	$\pm 1\sigma$
036JC01	268.89	441.05	0.61	0.05057	0.00429	0.25350	0.02101	0.03638	0.00076	221.3	185.1	230.3	4.7	229.4	17.0
037JC02	212.52	286.90	0.74	0.05082	0.00482	0.25233	0.02340	0.03603	0.00082	232.7	205.0	228.2	5.1	228.5	19.0
038JC03	207.62	303.20	0.68	0.05144	0.00463	0.25807	0.02272	0.03640	0.00080	260.7	194.3	230.5	5.0	233.1	18.3
039JC04	187.79	239.94	0.78	0.05103	0.00436	0.26083	0.02181	0.03709	0.00079	242.1	185.7	234.8	4.9	235.3	17.6
040JC05	238.62	478.69	0.50	0.05414	0.00309	0.27337	0.01526	0.03664	0.00059	376.9	123.3	232.0	3.7	245.4	12.2
041JC06	198.16	462.52	0.43	0.04954	0.00356	0.25175	0.01770	0.03688	0.00068	173.3	159.5	233.4	4.2	228.0	14.4
043JC07	201.05	491.76	0.41	0.05050	0.00347	0.25559	0.01718	0.03673	0.00066	218.0	151.6	232.5	4.1	231.1	13.9
044JC08	166.95	263.36	0.63	0.05161	0.00399	0.26115	0.01974	0.03672	0.00072	268.2	167.9	232.4	4.5	235.6	15.9
046JC10	225.20	433.85	0.52	0.04918	0.00253	0.25101	0.01265	0.03703	0.00055	156.5	116.2	234.4	3.4	227.4	10.3
047JC11	198.55	262.66	0.76	0.04962	0.00397	0.24770	0.01941	0.03622	0.00072	177.2	176.6	229.4	4.5	224.7	15.8
048JC12	254.81	354.23	0.72	0.05172	0.00387	0.25942	0.01900	0.03639	0.00070	273.2	162.9	230.4	4.4	234.2	15.3
052JC13	212.57	483.83	0.44	0.04967	0.00319	0.25286	0.01589	0.03694	0.00063	179.4	143.1	233.8	3.9	228.9	12.9
053JC14	281.16	492.65	0.57	0.04988	0.00288	0.25091	0.01420	0.03650	0.00058	189.4	129.2	231.1	3.6	227.3	11.5
054JC15	262.39	355.49	0.74	0.05133	0.00347	0.25826	0.01708	0.03650	0.00065	255.8	148.5	231.1	4.0	233.3	13.8
055JC16	243.22	280.10	0.87	0.04869	0.00354	0.24374	0.01733	0.03632	0.00067	133.0	162.4	230.0	4.1	221.5	14.2
056JC17	203.78	289.04	0.71	0.05205	0.00379	0.25822	0.01840	0.03600	0.00068	287.5	158.2	228.0	4.2	233.2	14.9
057JC18	261.62	436.59	0.60	0.05199	0.00283	0.26134	0.01392	0.03647	0.00057	284.8	119.9	230.9	3.5	235.7	11.2
059JC19	154.84	275.19	0.56	0.05147	0.00352	0.26143	0.01751	0.03685	0.00066	261.9	150.0	233.3	4.1	235.8	14.1
060JC20	199.47	306.07	0.65	0.05156	0.00419	0.25842	0.02052	0.03636	0.00074	266.0	176.1	230.2	4.6	233.4	16.6
061JC21	239.79	407.83	0.59	0.05067	0.00395	0.25414	0.01938	0.03639	0.00071	225.9	170.9	230.4	4.5	229.9	15.7
062JC22	225.72	366.96	0.62	0.05391	0.00304	0.27255	0.01502	0.03668	0.00059	367.0	121.8	232.2	3.7	244.7	12.0
063JC23	319.97	516.84	0.62	0.05049	0.00350	0.25658	0.01743	0.03687	0.00067	217.7	153.1	233.4	4.1	231.9	14.1
064JC24	247.69	379.15	0.65	0.05051	0.00335	0.25270	0.01639	0.03629	0.00064	218.6	146.5	229.8	4.0	228.8	13.3

表 3 浪麦滩正长花岗岩锆石微量元素($\times 10^{-6}$)测试结果

Table 3 Zircon trace elements ($\times 10^{-6}$) analysis result of Langmaitan syenogranite

测试点	La	Ce	Pr	Nd	Sm	Eu	Gd	Tb	Dy	Ho	Er	Tm	Yb	Lu
036JC01	0.00	26.80	0.16	2.42	4.40	0.05	29.81	11.01	135.02	50.63	227.45	42.46	380.82	61.85
037JC02	0.00	22.90	0.16	3.74	9.57	0.11	41.51	14.62	167.29	60.77	262.66	50.33	458.00	75.07
038JC03	0.11	26.08	0.15	3.11	4.21	0.02	27.77	10.87	126.07	47.58	195.79	37.69	344.96	60.57
039JC04	0.26	20.69	0.34	8.06	11.53	0.10	59.78	19.55	220.23	78.19	320.48	59.19	520.21	86.23
040JC05	0.14	24.00	0.12	1.35	4.09	0.32	28.09	12.22	143.76	54.82	246.29	49.26	435.04	70.96
041JC06	0.05	25.80	0.03	1.24	4.17	0.07	28.05	12.26	148.01	57.08	244.55	49.72	421.64	68.95
043JC07	0.01	24.59	0.07	1.23	4.19	0.02	24.04	10.14	134.07	53.01	231.90	48.46	404.18	66.10
044JC08	0.00	27.40	0.20	2.96	4.27	0.02	29.89	11.25	139.86	50.63	214.71	42.68	372.98	63.64
046JC10	0.01	24.80	0.04	1.45	4.14	0.15	25.08	10.68	124.36	47.65	212.36	40.74	369.49	61.23
047JC11	0.09	25.81	0.17	5.12	8.71	0.14	53.24	17.29	216.45	78.40	324.03	60.20	534.00	89.17
048JC12	0.10	22.91	0.17	6.19	10.52	0.11	56.69	20.51	232.44	92.97	370.10	71.86	637.75	99.18
052JC13	0.02	25.51	0.07	2.01	3.48	0.21	23.08	11.40	147.02	54.56	238.09	48.99	410.26	67.32
053JC14	0.00	28.29	0.14	1.23	5.23	0.18	28.90	11.14	145.91	53.96	232.76	46.39	409.48	63.97
054JC15	0.04	24.55	0.38	4.79	13.08	0.04	59.73	20.47	233.43	85.92	356.73	67.45	592.47	96.92
055JC16	0.04	13.77	0.49	8.87	14.87	0.23	74.31	24.92	289.81	100.67	406.15	79.82	690.58	116.25
056JC17	2.16	29.17	0.85	9.96	10.90	0.10	47.41	17.15	217.55	79.50	311.26	59.46	526.79	89.31
057JC18	0.12	27.46	0.18	1.07	5.81	0.06	29.65	11.21	145.73	53.12	227.99	43.86	387.70	62.33
059JC19	0.03	24.94	0.09	1.81	5.60	0.02	33.96	12.21	141.87	52.30	222.98	45.27	390.57	65.14
060JC20	0.00	22.78	0.11	2.62	5.81	0.05	35.84	11.85	145.77	53.17	230.79	44.44	408.15	72.04
061JC21	0.13	29.59	0.12	1.80	5.33	0.02	26.32	11.44	139.81	54.73	230.31	45.51	398.92	65.99
062JC22	0.00	27.46	0.10	2.08	6.25	0.03	33.91	11.28	142.91	53.47	226.66	46.27	408.58	68.57
063JC23	0.00	26.99	0.10	2.12	4.78	0.14	31.78	11.79	141.48	55.86	234.95	45.66	408.58	71.78
064JC24	0.00	30.37	0.14	2.34	6.27	0.06	31.82	12.70	153.91	57.56	243.11	47.23	424.66	68.52

3.4 Hf 同位素组成

正长花岗岩锆石 Hf 同位素数据见表 4。本次共选择 5 颗典型锆石进行 Lu-Hf 同位素测试, $^{176}\text{Yb}/^{177}\text{Hf}$ 比值介于 0.050150~0.090690 之间, $^{176}\text{Lu}/^{177}\text{Hf}$ 比值介于 0.001323~0.002529 之间,

$^{176}\text{Hf}/^{177}\text{Hf}$ 比值介于 0.282695~0.282849 之间; $\epsilon_{\text{Hf}}(t)$ 值介于 +2.05~+7.53 之间, 平均为 +5.35 (图 7); T_{DM1} 为 585~810 Ma, 平均 674 Ma; 二阶段 Hf 模式年龄 T_{DM2} 介于 782~1132 Ma 之间, 平均 922 Ma。

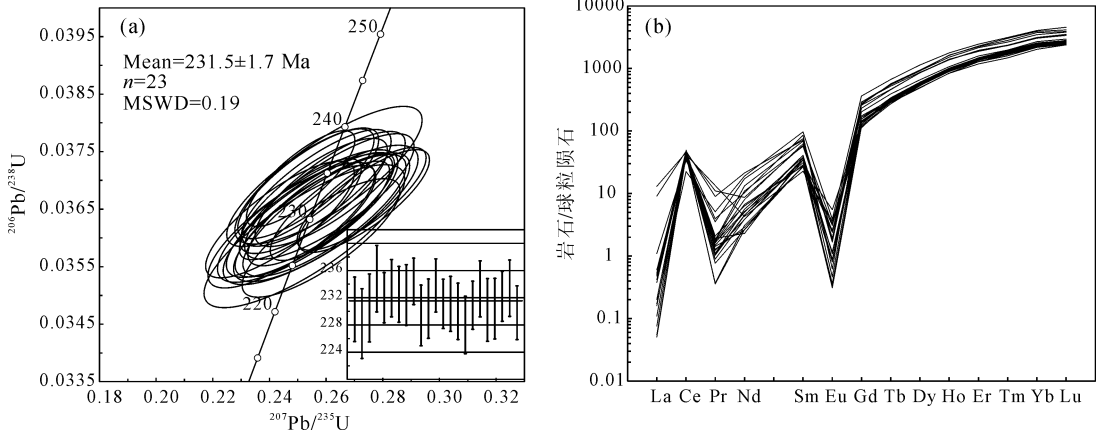


图 6 浪麦滩正长花岗岩锆石 U-Pb 年龄谱和图(a)及锆石稀土配分模式图(b)

Fig. 6 Zircon U-Pb concordia diagram (a) and chondrite-normalized rare earth element patterns (b) from Langmaitan syenogranite

表 4 浪麦滩正长花岗岩锆石 Hf 同位素

Table 4 Zircon in situ Hf isotope analysis data of Langmaitan syenogranite

点号	$t(\text{Ma})$	$^{176}\text{Yb}/^{177}\text{Hf}$	$^{176}\text{Lu}/^{177}\text{Hf}$	$\pm 2\sigma$	$^{176}\text{Hf}/^{177}\text{Hf}$	$\pm 2\sigma$	Hf_i	$\epsilon_{\text{Hf}}(t)$	$T_{\text{DM1}}(\text{Ma})$	$T_{\text{DM2}}(\text{Ma})$
1-JC3	231.5	0.074515	0.001949	0.000004	0.282849	0.000049	0.28284	7.53	585	782
2-JC7	231.5	0.090690	0.002529	0.000042	0.282803	0.000055	0.28279	5.80	663	893
3-JC12	231.5	0.070238	0.001860	0.000011	0.282817	0.000045	0.28281	6.40	631	855
4-JC17	231.5	0.050150	0.001323	0.000006	0.282774	0.000045	0.28277	4.95	683	947
5-JC22	231.5	0.077989	0.001975	0.000056	0.282695	0.000048	0.28269	2.05	810	1132

4 讨论

4.1 岩石成因类型

前人根据花岗岩的岩相学, 岩石地球化学等特征将其划分为 I、S、A、M 型 (Whalen et al., 1987; Chappell and White, 1992; Eby and Nelson, 1992; Clemens, 2003; Foden et al., 2015)。M 型花岗岩类岩石组合上多为辉长岩和闪长岩系列, 来自俯冲洋壳或者地幔楔熔融, 经广泛的分离结晶作用, 并且具有低含量的 Rb、Zr、REE 等地球化学特征 (Clemens, 2003)。浪麦滩正长花岗岩未见与之共生的中性岩类, 在南部出露有辉长岩, 其形成年龄为 $262.5 \pm 2.5 \text{ Ma}$ (Kong Huilei et al., 2017), 远早于浪麦滩正长花岗岩形成时间 ($231.5 \pm 1.7 \text{ Ma}$), 时间跨度大于 30 Ma, 不可能为 M 型花岗岩。Chappell and White (1992) 认为 $A/\text{CNK} = 1.1$ 可以作为划分 I 型和 S 型花岗岩的指标, S 型花岗岩

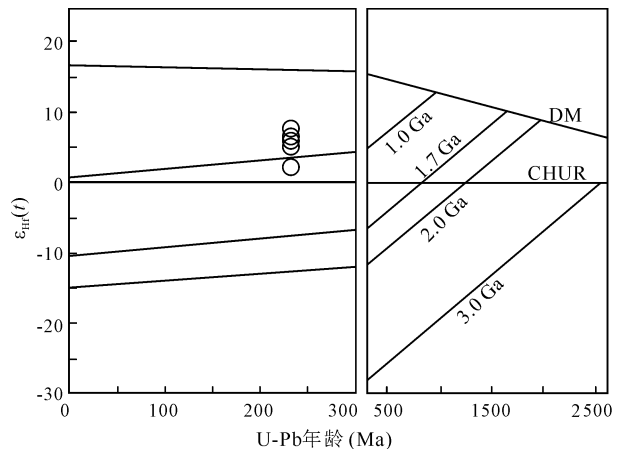


图 7 浪麦滩正长花岗岩 $\epsilon_{\text{Hf}}(t)$ -年龄图解

Fig. 7 $\epsilon_{\text{Hf}}(t)$ -age diagram of Langmaitan syenogranite

一般 A/CNK 比值大于 1.1, 而 I 型花岗岩 A/CNK 比值小于 1.1。浪麦滩正长花岗岩具有弱过铝质特征, A/CNK 值小于 1.0 (图 3d), 这些地球化学特征

与 S 型花岗岩特征不符,同时矿物组合上也没有 S 型花岗岩典型的富 Al 矿物,因此不可能是 S 型花岗岩(Chappell and White,1992)。

A 型花岗岩形成具有较高的温度,多由无水相矿物组成,如碱性矿物霓石、钠铁闪石,而 I 型花岗岩通常具有黑云母、角闪石等矿物分离结晶(King et al., 1997; Ma et al., 2018)。在矿物组合中,未见浪麦滩正长花岗岩含有角闪石等镁铁质矿物,与 I 型花岗岩也不符合。A 型花岗岩具有高硅高钾、低 Al 和 Sr 特征,与 I 型花岗岩的区别在于通常具有高的高场强元素含量,亏损 Sr、Ba、Cr、Co、Ni、V 和 Eu 元素等(Whalen et al., 1987)。浪麦滩正长花岗岩全岩具有低的 TiO_2 、MgO 等含量,较高的稀土总量,微量元素具有高的 Zr、Nb、Y 和 Ce 含量,相对富集 Rb、K、Th、U 等大离子亲石元素,亏损 Ba、Sr、Ti 等元素,具有高 Rb 含量($158 \times 10^{-6} \sim 189 \times 10^{-6}$),表明更可能为 A 型花岗岩而非 I 型;其 $\text{Zr} + \text{Nb} + \text{Ce} + \text{Y}$ 值大于 350,在 $(\text{Zr} + \text{Nb} + \text{Ce} + \text{Y}) - (\text{K}_2\text{O} + \text{Na}_2\text{O})/\text{CaO}$ 图解和在 $(\text{Zr} + \text{Nb} + \text{Ce} + \text{Y}) - \text{TFeO}/\text{MgO}$ 图解中全部落入 A 型花岗岩区域(Whalen et al., 1987)(图 8a、b);样品 $10^4 \times \text{Ga}/\text{Al}$

值介于 3.27~3.74,平均为 3.54,高于 A 型花岗岩判定标准 $10^4 \times \text{Ga}/\text{Al} = 2.6$,符合 A 型花岗岩特征(图 8c、d)。上述岩相学及地球化学特征均与 A 型花岗岩相似,表明浪麦滩正长花岗岩为 A 型花岗岩。

4.2 岩石成因

花岗岩 I、S、A、M 型划分方案广泛应用于岩石成因研究中(Whalen et al., 1987; Eby, 1990),其中针对 A 型花岗岩的成因主要有以下几种:① 各种源岩的部分熔融,如高温($>960^\circ\text{C}$)麻粒岩相变质岩(Collins et al., 1982; Huang et al., 2011),或残留下地壳花岗质岩石部分熔融(Collins et al., 1982; King et al., 1997);② 来自地幔玄武质岩浆分离结晶的产物(Litvinovsky et al., 2002; Mushkin et al., 2003);③ 上地壳钙碱性岩石低压熔融(Douce, 1997);④ 壳幔岩浆混合作用(Wickham et al., 1996; Yang et al., 2006; Zhang Qi et al., 2012; Ma et al., 2018)等。浪麦滩正长花岗岩未见与玄武质岩石共生,因此不太可能是地幔玄武质岩浆分异结晶的产物;在 $\epsilon_{\text{Hf}}(t) - T$ 图解中(图 7),样品点位于亏损地幔与球粒陨石演化线之间,二阶段 Hf 模式年

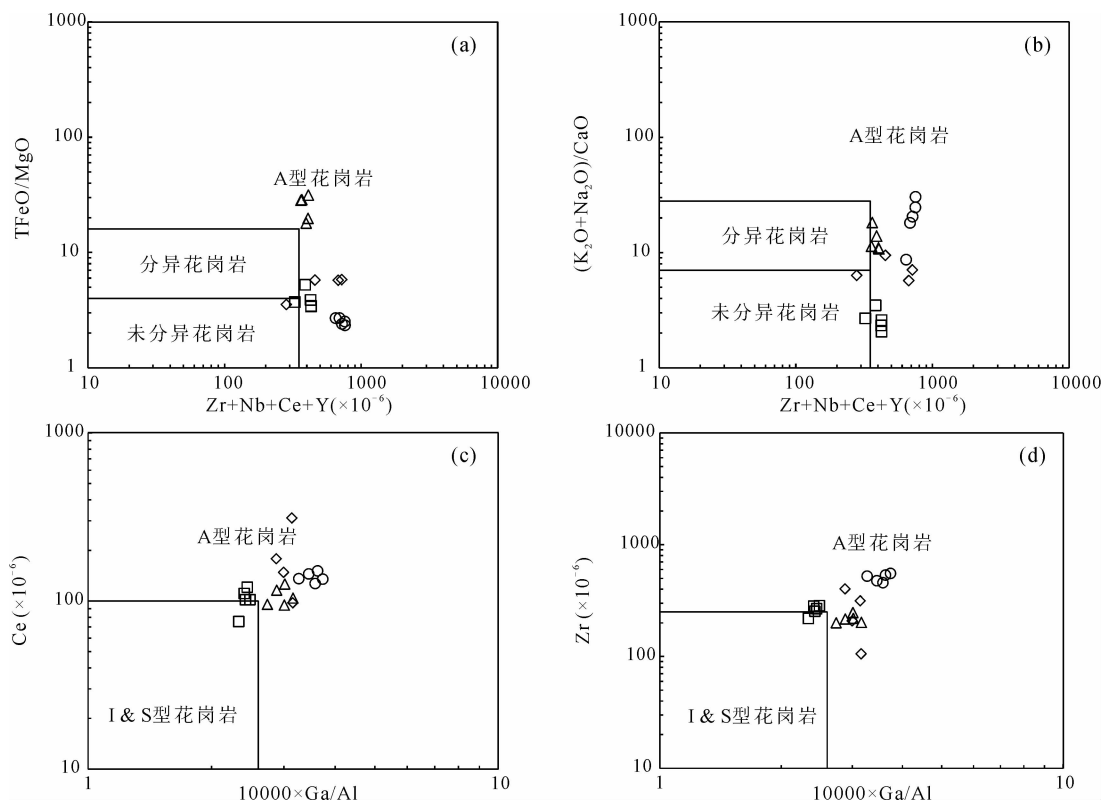


图 8 浪麦滩正长花岗岩成因类型判别图解(底图据 Whalen et al., 1987;图例同图 3)

Fig. 8 Discrimination diagrams for the genetic types of Langmaitan syenogranite (after Whalen et al., 1987; legends are the same as Fig. 3)

龄 T_{DM2} 介于 782~1132 Ma 之间,显示其具有新生地壳演化趋势,不太可能为上地壳钙碱性岩石低压熔融形成;由此可见浪麦滩正长花岗岩可能由来自各种源岩的部分熔融或壳幔混合作用形成。

浪麦滩正长花岗岩微量元素特征显示富集大离子亲石元素 Rb、Ba 等,亏损高场强元素 Nb、Ta、Ti,表明其源区可能主要来自地壳;样品的 Rb/Nb 比值为 4.47~5.25,与地壳相应比值 5.36~6.55 较为接近,而明显高于地幔相应比值 0.24~0.89;样品中 Nb 含量($34.6 \times 10^{-6} \sim 40.9 \times 10^{-6}$)和 Ta 含量($2.31 \times 10^{-6} \sim 2.91 \times 10^{-6}$)高于地壳岩石 Nb ($8 \times 10^{-6} \sim 11.5 \times 10^{-6}$)和 Ta ($0.7 \times 10^{-6} \sim 0.92 \times 10^{-6}$)含量值;样品 Nb/Ta 比值(13.52~15.58)介于下地壳 Nb/Ta 比值 10 与原始地幔 Nb/Ta 比值 17.5 之间,表明有幔源物质的参与。同时这也得到 Hf 同位素证据的支持, $\epsilon_{Hf}(t)$ 较高者通常指示其直接来自地幔或有幔源物质分异的新生壳源物质,而低 $\epsilon_{Hf}(t)$ 岩石表明源区往往为地壳或是经过地壳的混染作用。浪麦滩正长花岗岩 $\epsilon_{Hf}(t)$ 值在 +2.05~+7.53 之间,均为正值,并且相对变化范围大,暗示源区不均一性,可能有幔源物质的贡献。

幔源物质参与花岗质熔体的岩浆作用有两种方式,一种为幔源岩浆与壳源岩浆混合,另一种为幔源岩浆底侵形成新生地壳与古老地壳作为混合源区的部分熔融。项目组在野外填图过程中,未见正长花岗岩发育暗色微粒包体; $Mg^{\#}$ 值可以指示壳源岩浆作用是否有幔源物质的参与(Frost, 2001),浪麦滩正长花岗岩样品显示具有低的 MgO 值(0.81%~0.88%)特征, $Mg^{\#}$ 介于 0.40~0.43 之间,高于纯基性下地壳部分熔融产生的熔体($Mg^{\#}$ 值小于 40; Rapp and Watson, 1995),暗示具有幔源岩浆的贡献;岩石具有相对较高的 SiO_2 含量(72.36%~74.58%),较低的 Cr ($3.68 \times 10^{-6} \sim 47.6 \times 10^{-6}$)、Ni ($0.91 \times 10^{-6} \sim 17.8 \times 10^{-6}$)含量,Cr 含量远低于地幔橄榄岩源区部分熔融形成的原始玄武质岩浆($Cr = 500 \times 10^{-6} \sim 600 \times 10^{-6}$, Wilson, 1989),表明源区主要来自壳源岩浆。基于上述讨论,浪麦滩正长花岗岩应是有幔源岩浆贡献的新生下地壳部分熔融的产物。这种作用由于幔源岩浆底侵,导致新生地壳部分熔融并混入底侵的幔源物质,幔源的高温玄武质岩浆底侵新生下地壳,不仅为其部分熔融提供热源,同时还提供了少量物质,因此在地球化学特征上主要表现为壳源特征,同时也有幔源物质的信息。

4.3 构造环境

东昆仑作为特提斯构造演化的一部分,从晚泥盆世一早石炭世开始,东昆仑地块与巴颜喀拉地块之间经历了板块裂解拼和、洋陆转换、古特提斯洋的打开,至二叠纪一晚三叠世经历了洋壳扩张—闭合等演化过程(Yu et al., 2017; Dong et al., 2018; Xin et al., 2019)。蛇绿岩作为东昆仑古特提斯洋打开的标志,随后昆仑古特提斯洋北向俯冲,产生了大量与俯冲相关的花岗岩(Ma Changqian et al., 2015; Guo Xianzheng et al., 2018b; Chen et al., 2020)。前人对二叠纪—三叠纪大量花岗岩和镁铁质岩石进行了详细的岩相学、岩石地球化学和年代学研究,基本得出统一的认识,俯冲造山阶段主要发生在中晚二叠世到早三叠世(270~240 Ma),之后经历了碰撞—后碰撞造山。区域上中三叠世希里科特组与闹仓坚沟组存在角度不整合,且在 242~237 Ma,东昆仑的地层沉积环境由浅海相转变为河流相(Li Ruibao et al., 2012),以及存在约 244 Ma 清水泉角闪岩相同期高压变质作用记录;上述表明中晚三叠世时(~240 Ma)东昆仑古特提斯洋盆已经闭合,俯冲造山阶段结束,之后进入碰撞—后碰撞造山阶段。

花岗岩是地壳中最丰富的岩石之一,是地壳的重要组成部分,它记载了陆壳的形成、壳幔相互作用以及岩石圈演化的重要信息(Sengor et al., 1993; Taylor and McLennan, 1995; Petford et al., 2000; Mo Xuanxue, 2011; Zheng Yongfei and Chen Yixiang, 2019)。不同成因的花岗岩及其共生岩石组合能够反映不同的构造环境和地球动力学背景(Pearce et al., 1984; Maniar and Piccoli, 1989; Rudnick, 1995; Zhang Qi et al., 2007; Clemens and Stevens, 2012; Wang Tao et al., 2017)。本文获得浪麦滩 A 型花岗岩年龄 231.5 ± 1.7 Ma,结合前人在祁漫塔格地区获得 A 型花岗岩年龄为 210~218 Ma,上述 A 型花岗岩均晚于 237 Ma,表明可能形成于统一的碰撞—后碰撞构造背景。基于上述年代学,Shao Fengli (2017)在鄂拉山地区获得同期陆相火山岩流纹岩年龄 231.9 ± 1.6 Ma,认为其形成于后碰撞伸展环境;此外在东昆仑造山带出露同时期的与碰撞—后碰撞伸展构造背景有关的基性岩墙群(Liu et al., 2017)和镁铁—超镁铁岩,如小尖山辉长岩(Ao Cong et al., 2015);后碰撞伸展相关的高 Nb-Ta 流纹岩(Ding Shuo et al., 2011)以及埃达克质花岗岩(Feng Chengyou et al., 2012; Shao et

al., 2017; Chen Guochao et al., 2019)等,上述均表明东昆仑造山带在晚三叠世已经进入后碰撞伸展构造阶段。

A型花岗岩又可划分为A1和A2两个亚类,这两种类型花岗岩指示不同的构造环境(Gao et al., 2017; Shao et al., 2017; Chen et al., 2020)。A1型花岗岩代表了一种非造山环境,形成大陆裂谷时期或板内岩浆作用(如热点、地幔柱的活动);A2型形成的构造环境范围比较广泛,陆边缘伸展、陆内剪切相关的伸展、或是后碰撞伸展环境。通常A1型花岗岩具有低的Y/Nb (<1.2),而A2型花岗岩具有相对高的Y/Nb (>1.2)值,同时还有一些其他元素比值可以区分A1与A2型,如Rb/Nb、Ce/Nb、Yb/Ta等比值(Eby and Nelson, 1992),浪麦滩正长花岗岩Y/Nb均值为0.96,与A1型花岗岩特征基本一致。在A型花岗岩亚类Nb-Y-3Ga与Nb-Y-Ce判别图中(图9),浪麦滩正长花岗岩位于A1区域,同时搜集文献数据,区域于沟子钾长花岗岩也均落入A1区,而其他样品均位于A2区。同时代的A型花岗岩体不可能指示两种构造背景,说明该判别图解并不能全面指示构造背景,而应是对源区物质组成的反映。这种现象,在诸多地区均有出现,如形成于同一时代的浙江外北山、青田等A型花岗岩体,在A型花岗岩亚类判别图解中A1与A2共存(Duan Zheng et al., 2017)。前人研究表明同一构造背景A型花岗岩A1与A2亚类共存现象,是由壳幔物质不同比例引起(Azer, 2006)。Bonin (2007)指出从陆内到大陆边缘的各种动力学背景都可以形成A型花岗岩,因此A型花岗岩形成的关键因素是伸展应力,即产于伸展构造背景中。结合微量元素特征,浪麦滩正长花岗岩在(Yb+Ta)-Rb和

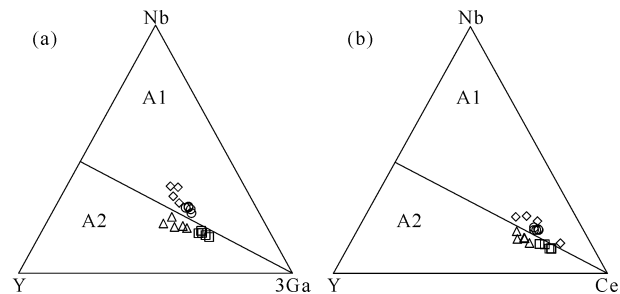


图9 浪麦滩正长花岗岩 Nb-Y-3Ga 和 Nb-Y-Ce 三角图解(底图据 Eby, 1990; 图例同图 3)

Fig. 9 Nb-Y-3Ga 和 Nb-Y-Ce ternary diagrams of the Langmaitan syenogranite (after Eby, 1990; legends are the same as Fig. 3)

(Y+Nb)-Rb 构造判别图解中落入后碰撞花岗岩区域(图10)。综上,本文认为浪麦滩A型花岗岩形成于晚三叠世后碰撞伸展背景。

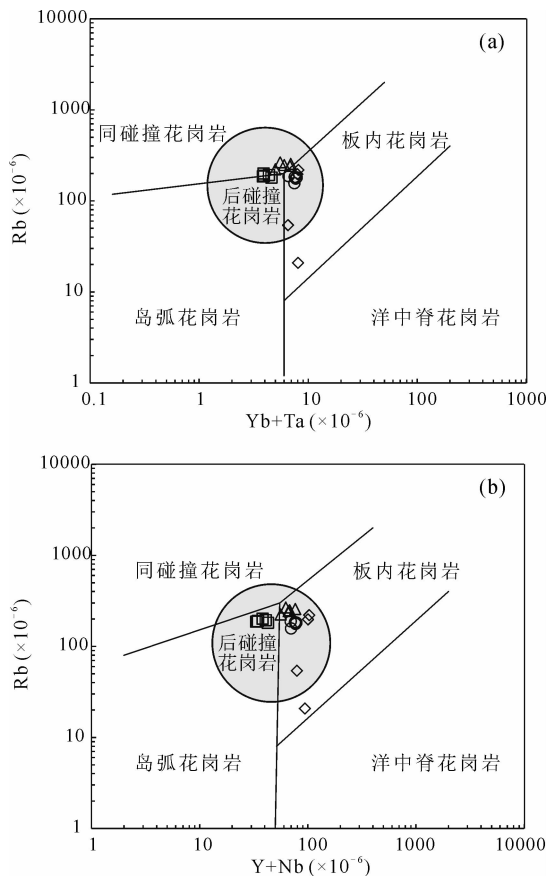


图10 浪麦滩正长花岗岩构造判别图解 (底图据 Pearce et al., 1984; 图例同 3)

Fig. 10 Discrimination diagrams of Langmaitan syenogranite (after Pearce et al., 1984; legends are the same as Fig. 3)

5 结论

(1)浪麦滩正长花岗岩 LA-ICP-MS 锆石 U-Pb 年龄为 231.5 ± 1.7 Ma, 形成时代为晚三叠世。

(2)岩相学、地球化学、Hf 同位素表明浪麦滩正长花岗岩为 A 型花岗岩,是由幔源物质贡献的新生下地壳部分熔融的产物。

(3)浪麦滩正长花岗岩形成于东昆仑古特提斯后碰撞伸展构造背景,表明东昆仑浪麦滩地区约 231 Ma 已进入伸展阶段。

References

- Anderson I C, Frost C D, Frost B R. 2003. Petrogenesis of the Red Mountain pluton, Laramie anorthosite complex, Wyoming: implications for the origin of A-type granite. *Precambrian Research*, 124(2): 243~267.
- Ao Cong, Sun Fengyue, Li Bile, Wang Guan, Li Liang, Li Shijin,

- Zhao Junwei. 2015. U-Pb dating, geochemistry and tectonic implications of Xiaojianshan gabbro in Qimantage Mountain, eastern Kunlun orogenic belt. *Geotectonica et Metallogenia*, 39 (6): 1176~1184 (in Chinese with English abstract).
- Azer M K. 2006. The petrogenesis of late Precambrian felsic alkaline magmatism in south Sinai, Egypt. *Acta Geologica Polonica*, 56(4): 463~484.
- Bonin B. 2007. A-type granites and related rocks: evolution of a concept, problems and prospects. *Lithos*, 97(1): 1~29.
- Bouvier A, Vervoort J D, Patchett P J. 2008. The Lu-Hf and Sm-Nd isotopic composition of CHUR: constraints from unequilibrated chondrites and implications for the bulk composition of terrestrial planets. *Earth and Planetary Science Letters*, 273(1/2): 48~57.
- Chappell B W, White A J R. 1992. I- and S-type granites in the Lachlan Fold Belt. *Transactions of the Royal Society of Edinburgh*, 83(1-2): 1~26.
- Chen Danling, Liu Liang, Che Zicheng, Luo Jinhai, Zhang Yunxiang. 2001. Determination and preliminary study of Indosinian aluminous A-type granites in the Qimantag area, southeastern Xinjiang. *Geochimica*, 30 (6): 540 ~ 546 (in Chinese with English abstract).
- Chen Guochao, Li Xiaobing, Pei Xianzhi, Li Ruibao, Li Zuocheng, Pei Lei, Liu Chengjun, Chen Youxi, Wang Meng, Gao Feng. 2019. Lithospheric extension of the post-collision stage of the Paleo-Tethys oceanic system in the East Kunlun orogenic belt: insights from Late Triassic plutons. *Earth Science Frontiers*, 26 (4): 191~208 (in Chinese with English abstract).
- Chen Jiajie, Fu Lebing, Wei Junhao, Selby D, Zhang Daohan, Zhou Hongzhi, Zhao Xu, Liu Yan. 2020. Proto-Tethys magmatic evolution along northern Gondwana: insights from Late Silurian-Middle Devonian A-type magmatism, East Kunlun orogen, northern Tibetan Plateau, China. *Lithos*, 356 ~ 357: 105304.
- Clemens J D. 2003. S-type granitic magmas—petrogenetic issues, models and evidence. *Earth-Science Reviews*, 61(1): 1~18.
- Clemens J D, Stevens G. 2012. What controls chemical variation in granitic magmas? *Lithos*, 134~135: 317~329.
- Collins W J, Beams S D, White A J R, Chappell B W. 1982. Nature and origin of A-type granites with particular reference to southeastern Australia. *Contributions to Mineralogy & Petrology*, 80(2): 189~200.
- Ding Shuo, Huang Hui, Niu Yaoling, Zhao Zhidan, Yu Xuehui, Mo Xuanxue. 2011. Geochemistry, geochronology and petrogenesis of East Kunlun high Nb-Ta rhyolites. *Acta Petrologica Sinica*, 27(12): 3603~3614 (in Chinese with English abstract).
- Dong Yunpeng, He Dengfeng, Sun Shengsi, Liu Xiaoming, Zhou Xiaohu, Zhang Feifei, Yang Zhao, Cheng Bin, Zhao Guochun, Li Jianhua. 2018. Subduction and accretionary tectonics of the East Kunlun orogen, western segment of the Central China Orogenic System. *Earth-Science Reviews*, 186: 231~261.
- Douce A E P. 1997. Generation of metaluminous A-type granites by low-pressure melting of calc-alkaline granitoids. *Geology*, 25 (8): 743.
- Duan Zheng, Xing Guangfu, Yu Minggang, Zhao Xilin, Jin Guodong. 2017. The petrogenesis of Waibeishan aluminous A₁ type granite in Zhejiang Province: constraints from mineralogy, zircon U-Pb dating, geochemistry and Hf isotope. *Acta Geologica Sinica*, 91(1): 180~197 (in Chinese with English abstract).
- Eby G N. 1990. The A-type granitoids: a review of their occurrence and chemical characteristics and speculations on their petrogenesis. *Lithos*, 26(1): 115~134.
- Eby G N, Nelson G. 1992. Chemical subdivision of the A-type granitoids: petrogenetic and tectonic implications. *Geology*, 20 (7): 641.
- Feng Chengyou, Wang Song, Li Guocheng, Ma Shensha, Li Dongsheng. 2012. Middle to Late Triassic granitoids in the Qimantage area, Qinghai Province, China: chronology, geochemistry and metallogenic significances. *Acta Petrologica Sinica*, 28(2): 665~678 (in Chinese with English abstract).
- Foden J, Sossi P A, Wawryk C M. 2015. Fe isotopes and the contrasting petrogenesis of A-, I- and S-type granite. *Lithos*, 212~215: 32~44.
- Frost B R. 2001. Ageochemical classification for granitic rocks. *Journal of Petrology*, 42(11): 2033~2048.
- Gao Peng, Zheng Yongfei, Zhao Zifu. 2017. Triassic granites in South China: a geochemical perspective on their characteristics, petrogenesis, and tectonic significance. *Earth-Science Reviews*, 266~294.
- Gao Yongbao, Li Wenyuan, Qian Bing, Li Kan, Li Dongsheng, He Shuyue, Zhang Zhaowei, Zhang Jiangwei. 2014. Geochronology, geochemistry and Hf isotopic compositions of the granitic rocks related with iron mineralization in Yemaquan deposit, East Kunlun, NW China. *Acta Petrologica Sinica*, 30 (6): 1647~1665 (in Chinese with English abstract).
- Griffin W L, Pearson N J, Belousova E, Jackson S E, Achterbergh E V, O'Reilly S Y, Shee S R. 2000. The Hf isotope composition of cratonic mantle: LAM-MC-ICPMS analysis of zircon megacrysts in kimberlites. *Geochimica et Cosmochimica Acta*, 64(1): 133~147.
- Guo Xianzheng, Jia Qunzi, Li Jinchao, Kong Huilie, Yao Xuegang, Mi Jiaru, Qian Bing, Wang Yu. 2018a. Zircon U-Pb geochronology and geochemistry and their geological significances of eclogites from East Kunlun high-pressure metamorphic belt. *Earth Science*, 43(12): 36~54 (in Chinese with English abstract).
- Guo Xianzheng, Li Yazhi, Jia Qunzi, Li Jinchao, Kong Huilei, Namkha Norbu. 2018b. Geochronology and geochemistry of the Wulonggou orefield related granites in Late Permian-Triassic East Kunlun: implication for metallogenic tectonic. *Acta Petrologica Sinica*, 34(8): 2359~2379 (in Chinese with English abstract).
- Guo Xianzheng, Xie Wanhong, Zhou Hongbing, Tian Chengsheng, Li Jinchao, Kong Huilei, Yang Tao, Yao Xuegang, Jia Qunzi. 2019a. Zircon U-Pb chronology and geochemistry of the rhyolite porphyry in the Nagengkangqieer silver polymetallic deposit, East Kunlun and their geological significance. *Earth Science*, 44 (7): 2505~2528 (in Chinese with English abstract).
- Guo Xianzheng, Jia Qunzi, Li Jinchao, Kong Huilei, Yao Xuegang, Li Yazhi. 2019b. Geochronology and geochemical characteristics of syenogranite from the Zhamaxiuma area in east Kunlun and their tectonic significance. *Acta Geologica Sinica*, 93(04): 70~82 (in Chinese with English abstract).
- Hoskin P W O, Schaltegger U. 2003. The composition of zircon and igneous and metamorphic petrogenesis. *Reviews in Mineralogy and Geochemistry*, 53: 27~55.
- Huang Huiqing, Li Xianhua, Li Wuxian, Li Zhengxiang. 2011. Formation of high $\delta^{18}\text{O}$ fayalite-bearing A-type granite by high-temperature melting of granulitic metasedimentary rocks, southern China. *Geology*, 39(10): 903~906.
- Huang Hui, Wang Kaixing, Pan Jiayong, Liu Xiaodong, Sun Yue. 2019. A-type volcanic-intrusive complex in the Huanggangshan Basin: implications for early cretaceous crust-mantle interaction in the Gan-Hang Belt and adjacent areas, South China. *Lithos*, 336~337: 258~275.
- King P L, White A J R, Chappell B W, Allen C M. 1997. Characterization and origin of aluminous A-type granites from the Lachlan fold belt, southeastern Australia. *Journal of Petrology*, (3): 371~391.
- Kong Huilei, Li Jinchao, Li Yazhi, Jia Qunzi, Guo Xianzheng. 2017. Zircon LA-ICP-MS U-Pb dating and its geological significance of the Jiadang gabbro in the eastern section of East Kunlun, Qinghai Province. *Geology and Exploration*, 53(5): 889~902 (in Chinese with English abstract).
- Lei Ruxiong, Wu Changzhi, Chi Guoxiang, Gu Lianxing, Dong Lianhui, Qu Xun, Jiang Yaohui, Jiang Shaoyong. 2013. The Neoproterozoic Hongliujing A-type granite in Central Tianshan

- (NW China): LA-ICP-MS zircon U-Pb geochronology, geochemistry, Nd-Hf isotope and tectonic significance. *Journal of Asian Earth Sciences*, 74(25): 142~154.
- Li Guochen, Feng Chengyou, Wang Ruijiang, Ma Shengchao, Li Hongmao, Zhou Anshun. 2012. SIMS zircon U-Pb age, petrochemistry and tectonic implications of granitoids in northeastern Baiganhu W-Sn orefield, Xinjiang. *Acta Geoscientia Sinica*, 33(2): 216~226 (in Chinese with English abstract).
- Li Ruibao, Pei Xianzhi, Li Zuochen, Liu Zhanqing, Chen Guochao, Chen Youxin, Wei Fanghui, Gao Jingmin, Liu Chengjun, Pei Lei. 2012. Geological characteristics of Late Paleozoic-Mesozoic unconformities and their response to some significant tectonic events in eastern part of Eastern Kunlun. *Earth Science Frontiers*, 19(5): 244~254 (in Chinese with English abstract).
- Li Yanguang, Wang Shuangshuang, Liu Minwu, Meng En, Wei Xiaoyan, Zhao Huibo, Jin Mengqi. 2015. U-Pb dating study of baddeleyite by LA-ICP-MS: technique and application. *Acta Geologica Sinica*, 89(12): 2400~2418 (in Chinese with English abstract).
- Litvinovsky B A, Jahn B M, Zanvilevich A N, Saunders A, Titov A V. 2002. Petrogenesis of syenite-granite suites from the Bryansky complex (Transbaikalia, Russia): implications for the origin of A-type granitoid magmas. *Chemical Geology*, 189(1): 105~133.
- Liu Bin, Ma Changqian, Zhang Jinyang, Xiong Fuhao, Huang Jian, Jiang Hongan. 2012. Petrogenesis of Early Devonian intrusive rocks in the east part of eastern Kunlun orogen and implication for Early Palaeozoic orogenic processes. *Acta Petrologica Sinica*, 28(6): 1785~1807 (in Chinese with English abstract).
- Liu Bin, Ma Changqian, Huang Jian, Wang Lianxun, Zhao Shaoqing, Yan Rong, Sun Yang, Xiong Fuhao. 2017. Petrogenesis and tectonic implications of Upper Triassic appinite dykes in the East Kunlun orogenic belt, northern Tibetan Plateau. *Lithos*, 284~285: 766~778.
- Liu Lei, Qian Ye, Sun Fengyue, Li Yujin, Gu Yan, Zhang Jianping. 2019. Geochronology, geochemistry and technology of Late Devonian A-type granite in Qunli area, eastern Kunlun. *Global Geology*, 38(1): 34~45 (in Chinese with English abstract).
- Liu Yuegao, Li Wenyuan, Jia Qunzi, Zhang Zhaowei, Wang Zhian, Zhang Zhibing, Zhang Jiangwei, Qian Bing. 2018. The dynamic sulfide saturation process and a possible slab break-off model for the giant Xiarihamu magmatic nickel ore deposit in the East Kunlun orogenic belt, northern Qinghai-Tibet Plateau, China. *Economic Geology*, 113(6): 1383~1417.
- Loiselle M C. 1979. Characteristics and origin of anorogenic granites. *Geological Society of America Abstracts with Programs*, 11: 468.
- Ma Changqian, Xiong Fuhao, Yin Shuo, Wang Lianxun, Gao Ke. 2015. Intensity and cyclicity of orogenic magmatism: an example from a Paleo-Tethyan granitoid batholith, Eastern Kunlun, northern Qinghai-Tibetan Plateau. *Acta Petrologica Sinica*, 31(12): 3555~3568 (in Chinese with English abstract).
- Ma Lin, Kerr A C, Wang Qiang, Jiang Ziqi, Hu Wanlong. 2018. Early Cretaceous (similar to 140 Ma) aluminous A-type granites in the Tethyan Himalaya, Tibet: products of crust-mantle interaction during lithospheric extension. *Lithos*, 300: 212~226.
- Mani P D, Piccoli P M. 1989. Tectonic discrimination of granitoids. *Geological Society of America Bulletin*, 101(5): 635~643.
- Middlemost E A K. 1994. Naming materials in the magma/igneous rock system. *Earth-Science Reviews*, 37(3): 215~224.
- Mo Xuanxue. 2011. Magmatism and evolution of the Tibetan Plateau. *Geological Journal of China Universities*, 17(3): 351~367 (in Chinese with English abstract).
- Mo Xuanxue, Luo Zhaohua, Deng Jinfu, Yu Xuehui, Liu Chengdong, Chen Hongwei, Yuan Wanming, Liu Yunhua. 2007. Granitoids and crustal growth in the East-Kunlun orogenic belt. *Geological Journal of China Universities*, 13(3): 403~414 (in Chinese with English abstract).
- Mushkin A, Navon O, Halicz L, Hartmann G, Stein M. 2003. The petrogenesis of A-type magmas from the Amrammassif, southern Israel. *Journal of Petrology*, 44(5): 815~832.
- Pearce J A, Harris N B W, Tindle A G. 1984. Trace element discrimination diagrams for the tectonic interpretation of granitic rocks. *Journal of Petrology*, 25(4): 956~983.
- Peccerillo A, Taylor S R. 1976. Geochemistry of Eocene calc-alkaline volcanic rocks from the Kastamonu area, northern Turkey. *Contributions to Mineralogy and Petrology*, 58(1): 63~81.
- Petford N, Cruden A R, McCaffrey K J, Vigneresse J L. 2000. Granite magma formation, transport and emplacement in the Earth's crust. *Nature*, 408(6813): 669~673.
- Qian Bing, Gao Yongbao, Li Kan, Zhang Zhaowei, Zhou Anshun, Wu Yushi. 2015. Zircon U-Pb-Hf isotopes and whole rock geochemistry constraints on the petrogenesis of iron-rare metal mineralization related alkaline granitic intrusive rock in Yugouzi area, eastern Kunlun, Xinjiang. *Acta Petrologica Sinica*, 31(9): 2508~2520 (in Chinese with English abstract).
- Rapp R P, Watson E B. 1995. Dehydration melting of metabasalt at 8-32 kbar: implications for continental growth and crust-mantle recycling. *Journal of Petrology*, 36: 891~931.
- Rudnick R L. 1995. Making continental crust. *Nature*, 378(6557): 571~578.
- Söderlund U, Patchett P J, Vervoort J D, Isachsen C E. 2004. The ¹⁷⁶Lu decay constant determined by Lu-Hf and U-Pb isotope systematics of Precambrian mafic intrusions. *Earth and Planetary Science Letters*, 219(3-4): 311~324.
- Sengor A M C, Natal'in B A, Burtman V S. 1993. Evolution of the Altaid tectonic collage and Palaeozoic crustal growth in Eurasia. *Nature*, 54(6435): 117~137.
- Shao Fengli. 2017. Petrogenesis of Triassic granitoids and rhyolites in the East Kunlun orogenic belt and their tectonic implications. Doctoral thesis of University of Chinese Academy of Sciences (in Chinese with English abstract).
- Shao Fengli, Niu Yaoling, Liu Yi, Chen Shuo, Kong Juanjuan, Duan Meng. 2017. Petrogenesis of Triassic granitoids in the East Kunlun orogenic belt, northern Tibetan Plateau and their tectonic implications. *Lithos*, 282~283: 33~44.
- Song Xieyan, Yi Junnian, Chen Liemeng, She Yuwei, Liu Changzheng, Dang Xingyan, Yang Qian, Wu Shukuan. 2016. The giant Xiarihamu Ni-Co sulfide deposit in the East Kunlun orogenic belt, northern Tibet Plateau, China. *Economic Geology*, 111(1): 29~55.
- Sun S S, McDonough W F. 1989. Chemical and isotopic systematics of oceanic basalts: implications for mantle composition and processes. *Geological Society London Special Publications*, 42(1): 313~345.
- Taylor S, McLennan S. 1995. The geochemical evolution of the continental crust. *Reviews of Geophysics*, 33(2): 241~265.
- Wang Guan, Sun Fengyue, Li Bile, Li Shijin, Zhao Junwei, Yang Qi'an, Ao Cong. 2013. Zircon U-Pb geochronology and geochemistry of the Early Devonian syenogranite and the Xiarihamu ore district from East Kunlun, with implications for the geodynamic setting. *Geotectonica et Metallogenia*, 37(4): 127~139 (in Chinese with English abstract).
- Wang Tao, Wang Xiaoxia, Guo Lei, Zhang Lei, Tong Yin, Li Shan, Huang He, Zhang Jianjun. 2017. Granitoid and tectonics. *Acta Petrologica Sinica*, 33(5): 1459~1478 (in Chinese with English abstract).
- Whalen J, Currie K, Chappell B. 1987. A-type granites: geochemical characteristics, discrimination and petrogenesis. *Contributions to Mineralogy and Petrology*, 95(4): 407~419.
- Wickham S M, Alberts A D, Zanvilevich A N, Litvinovsky B A,

- Bindeman I, Schauble E A. 1996. A stable isotope study of anorogenic magmatism in East Central Asia. *Journal of Petrology*, 37(5): 1063~1095.
- Wilson M. 1989. *Igneous Petrogenesis: a Global Tectonic Approach*. London: Unwin Hyman, 1~466.
- Xia Rui, Wang Changming, Qing Min, Li Wenliang, Carranza E J M, Guo Xiaodong, Ge Liangsheng, Zeng Guanzhong. 2015. Zircon U-Pb dating, geochemistry and Sr-Nd-Pb-Hf-O isotopes for the Nan'getan granodiorites and mafic microgranular enclaves in the East Kunlun orogen: record of closure of the Paleo-Tethys. *Lithos*, 234~235: 47~60.
- Xin Wei, Sun Fengyue, Zhang Yuting, Fan Xingzhu, Wang Yingchao, Li Liang. 2019. Mafic-intermediate igneous rocks in the East Kunlun orogenic belt, northwestern China: Petrogenesis and implications for regional geodynamic evolution during the Triassic. *Lithos*, 346~347: 105159.
- Xu Zhiqin, Li Haibing, Yang Jjinsui. 2006. An orogenic plateau-the orogenic collage and orogenic types of the Qinghai-Tibet plateau. *Earth Science Frontiers*, 13(4): 1~17 (in Chinese with English abstract).
- Yan Wei, Qiu Dianming, Ding Qingfeng, Liu Fei. 2016. Geochronology, petrogenesis, source and its structural significance of Houtougou monzogranite of Wulonggou area in eastern Kunlun orogen. *Journal of Jilin University (Earth Science Edition)*, 46(2): 443~460 (in Chinese with English abstract).
- Yang Jinhui, Wu Fuyuan, Chung Sunlin, Wilde Simona, Chu Meifei. 2006. A hybrid origin for the Qianshan A-type granite, northeast China: geochemical and Sr-Nd-Hf isotopic evidence. *Lithos*, 89(1): 89~106.
- Yao Xuegang, Zhou Shuai, Jia Qunzi, Li Jinchao, Kong Huilei, Guo Xianzheng, Wang Yu. 2018. Zircon U-Pb dating and geochemical characteristics of monzogranite in the Shengli iron-copper deposit form East Kunlun Mountains and its prospecting significance. *Geological Science and Technology Information*, 37(5): 11~20 (in Chinese with English abstract).
- Yu M, Feng C Y, Santosh M, Mao J W, Zhu Y F, Zhao Y M, Li D X, Li B. 2017. The Qiman Tagh orogen as a window to the crustal evolution in northern Qinghai-Tibet Plateau. *Earth-Science Reviews*, 167: 103~123.
- Yuan Honglin, Gao Shan, Dai Mengning, Zong Chunlei, Günther D, Fontaine G, Liu Xiaoming, Diwu Chunrong. 2008. Simultaneous determinations of U-Pb age, Hf isotopes and trace element compositions of zircon by excimer laser-ablation quadrupole and multiple-collector ICP-MS. *Chemical Geology*, 247(1-2): 100~118.
- Zhang Mingyu, Feng Chengyou, Wang Hui, Li Daxin, Ju Hongying, Liu Jiannan, Zhou Jianhou. 2018. Petrogenesis and tectonic implications of the Late Triassic syenogranite in Qimantag area, East Kunlun Mountains. *Acta Petrologica et Mineralogica*, 37(2): 197~210 (in Chinese with English abstract).
- Zhang Qi, Pan Guoqiang, Li Chengdong, Jin Weijun, Jia Xiuqin. 2007. Are discrimination diagram always indicative of correct tectonic settings of granite? Some crucial question on granite study (3). *Acta Petrologica Sinica*, 23(11): 2683~2698 (in Chinese with English abstract).
- Zhang Qi, Ran Hao, Li Chengdong. 2012. A-type granite: what is the essence? *Acta Petrologica et Mineralogica*, 31(4): 621~626 (in Chinese with English abstract).
- Zhang Zhaowei, Li Wenyuan, Qian Bing, Wang Yalei, Li Shijin, Liu Zhangzheng, Zhang Jiangwei, Yang Qi'an, You Minxin, Wang Zhi'an. 2015. Metallogenic epoch of the Xiarihamu magmatic Ni-Cu sulfide deposit in eastern Kunlun orogenic belt and its prospecting significance. *Geology in China*, 42(03): 438~451 (in Chinese with English abstract).
- Zheng Yongfei, Chen Yixiang. 2019. Crust-mantle interaction in continental subduction zones. *Earth Science*, 44(12): 3961~3983 (in Chinese with English abstract).

参 考 文 献

- 奥琮, 孙丰月, 李碧乐, 王冠, 李良, 李世金, 赵俊伟. 2015. 东昆仑祁漫塔格地区小尖山辉长岩地球化学特征、U-Pb年代学及其构造意义. *大地构造与成矿学*, 39(6): 1176~1184.
- 陈丹玲, 刘良, 车自成, 罗金海, 张云翔. 2001. 祁漫塔格印支期铝质A型花岗岩的确定及初步研究. *地球化学*, 30(6): 540~546.
- 陈国超, 李小兵, 裴先治, 李瑞保, 李佐臣, 裴磊, 刘成军, 陈有妍, 王盟, 高峰. 2019. 东昆仑古特提斯后碰撞阶段伸展作用: 来自晚三叠世岩浆岩的证据. *地学前缘*, 26(4): 191~208.
- 丁烁, 黄慧, 牛耀龄, 赵志丹, 喻学惠, 莫宣学. 2011. 东昆仑高Nb-Ta流纹岩的年代学、地球化学及成因. *岩石学报*, 27(12): 3603~3614.
- 段政, 邢光福, 余明刚, 赵希林, 靳国栋. 2017. 浙江外北山铝质A1型花岗岩成因: 矿物学、年代学、地球化学及Hf同位素制约. *地质学报*, 91(1): 180~197.
- 丰成友, 王松, 李国臣, 马圣钞, 李东生. 2012. 青海祁漫塔格中晚三叠世花岗岩: 年代学、地球化学及成矿意义. *岩石学报*, 28(2): 311~324.
- 高永宝, 李文渊, 钱兵, 李侃, 李东生, 何书跃, 张照伟, 张江伟. 2014. 东昆仑野马泉铁矿相关花岗岩体年代学、地球化学及Hf同位素特征. *岩石学报*, 30(6): 1647~1665.
- 国显正, 贾群子, 李金超, 孔会磊, 姚学钢, 陈佳茹, 钱兵, 王宇. 2018a. 东昆仑高压变质带榴辉岩年代学、地球化学及其地质意义. *地球科学*, 43(12): 36~54.
- 国显正, 栗亚芝, 贾群子, 李金超, 孔会磊, 南卡俄吾. 2018b. 东昆仑五龙沟金多金属矿集区晚二叠世—三叠纪岩浆岩年代学、地球化学及其构造意义. *岩石学报*, 34(8): 2359~2379.
- 国显正, 谢万洪, 周洪兵, 田承盛, 李金超, 孔会磊, 杨涛, 姚学钢, 贾群子. 2019a. 东昆仑那更康切尔银多金属矿床流纹斑岩锆石U-Pb年代学、地球化学特征及其地质意义. *地球科学*, 44(7): 2505~2518.
- 国显正, 贾群子, 李金超, 孔会磊, 姚学钢, 栗亚芝. 2019b. 东昆仑扎玛休玛正长花岗岩年代学、地球化学特征及其构造意义. *地质学报*, 93(04): 70~82.
- 孔会磊, 李金超, 栗亚芝, 贾群子, 国显正. 2017. 青海东昆仑东段加当辉长岩LA-ICP-MS锆石U-Pb测年及其地质意义. *地质与勘探*, 53(5): 889~902.
- 李国臣, 丰成友, 王瑞江, 马圣钞, 李洪茂, 周安顺. 2012. 新疆白干湖钨锡矿田东北部花岗岩锆石SIMS U-Pb年龄、地球化学特征及构造意义. *地球学报*, 33(2): 216~226.
- 李瑞保, 裴先治, 李佐臣, 刘战庆, 陈国超, 陈有妍, 魏方辉, 高景民, 刘成军, 裴磊. 2012. 东昆仑东段晚古生代—中生代若干不整合面特征及其对重大构造事件的响应. *地学前缘*, 19(5): 244~254.
- 李艳广, 汪双双, 刘民武, 孟恩, 魏小燕, 赵慧博, 靳梦琪. 2015. 斜锆石LA-ICP-MS U-Pb定年方法及应用. *地质学报*, 89(12): 2400~2418.
- 刘彬, 马昌前, 张金阳, 熊富浩, 黄坚, 蒋红安. 2012. 东昆仑造山带东段早泥盆世侵入岩的成因及其对早古生代造山作用的指示. *岩石学报*, 28(6): 1785~1807.
- 刘雷, 钱焯, 孙丰月, 李子晋, 顾焱, 张建平. 2019. 东昆仑群力地区晚泥盆世A型花岗岩的年代学、地球化学和构造意义. *世界地质*, 38(1): 34~45.
- 马昌前, 熊富浩, 尹烁, 王连训, 高珂. 2015. 造山带岩浆作用的强度和旋回性: 以东昆仑古特提斯花岗岩类岩基为例. *岩石学报*, 31(12): 3555~3568.
- 莫宣学. 2011. 岩浆作用与青藏高原演化. *高校地质学报*, 17(03): 351~367.
- 莫宣学, 罗照华, 邓晋福, 喻学惠, 刘成东, 谌宏伟, 袁万明, 刘云华. 2007. 东昆仑造山带花岗岩及地壳生长. *高校地质学报*, 13(3): 403~414.
- 钱兵, 高永宝, 李侃, 张照伟, 周安顺, 吴玉诗. 2015. 新疆东昆仑

于沟子地区与铁-稀有多金属成矿有关的碱性花岗岩地球化学、年代学及 Hf 同位素研究. 岩石学报, 31(9): 2508~2520.

邵凤丽. 2017. 东昆仑造山带三叠纪花岗岩类和流纹岩类的成因: 洋壳到陆壳的转化. 中国科学院大学博士学位论文.

王冠, 孙丰月, 李碧乐, 李世金, 赵俊伟, 杨启安, 奥琼. 2013. 东昆仑夏日哈木矿区早泥盆世正长花岗岩锆石 U-Pb 年代学、地球化学及其动力学意义. 大地构造与成矿学, 37(4): 127~139.

王涛, 王晓霞, 郭磊, 张磊, 童英, 李舫, 黄河, 张建军. 2017. 花岗岩与大地构造. 岩石学报, 33(5): 1459~1478.

许志琴, 李海兵, 杨经绥. 2006. 造山的高原——青藏高原巨型造山拼贴体和造山类型. 地学前缘, 13(4): 1~17.

严威, 邱殿明, 丁清峰, 刘飞. 2016. 东昆仑五龙沟地区猴头沟二长花岗岩年龄、成因、源区及其构造意义. 吉林大学学报(地球科学版), 46(2): 443~460.

姚学钢, 周帅, 贾群子, 李金超, 孔会磊, 国显正, 王宇. 2018. 东

昆仑胜利铁铜矿区二长花岗岩锆石 U-Pb 定年、岩石地球化学特征及找矿意义. 地质科技通报, 37(5): 11~20.

张明玉, 丰成友, 王辉, 李大新, 瞿泓滢, 刘建楠, 周建厚. 2018. 东昆仑祁漫塔格地区晚三叠世正长花岗岩岩石成因及构造意义. 岩石矿物学杂志, 37(2): 197~210.

张旗, 潘国强, 李承东, 金惟俊, 贾秀勤. 2007. 花岗岩构造环境问题: 关于花岗岩研究的思考之三. 岩石学报, 23(11): 2683~2698.

张旗, 冉焱, 李承东. 2012. A 型花岗岩的实质是什么?. 岩石矿物学杂志, 31(4): 621~626.

张照伟, 李文渊, 钱兵, 王亚磊, 李世金, 刘长征, 张江伟, 杨启安, 尤敏鑫, 王治安. 2015. 东昆仑夏日哈木岩浆铜镍硫化物矿床成矿时代的厘定及其找矿意义. 中国地质, 42(03): 438~451.

郑永飞, 陈伊翔. 2019. 大陆俯冲带壳幔相互作用. 地球科学, 44(12): 3961~3983.

Geochronology, geochemical characteristics and geological significance of A-type granite from the Langmaitan area, East Kunlun

LI Jinchao¹⁾, GUO Xianzheng^{*2)}, KONG Huilei¹⁾, YAO Xuegang¹⁾, JIA Qunzi¹⁾

1) Xi'an Center of Geological Survey, CGS, Key Laboratory for the Study of Focused Magmatism and Giant Ore Deposit, MNR, Xi'an, Shaanxi 710054, China;

2) School of Resources and Environmental Engineering, Hefei University of Technology, Hefei, Anhui 230009, China

* Corresponding author: cuggxz@126.com

Abstract

East Kunlun contains large areas of intermediate-acid intrusive rocks, providing a natural laboratory for the study of magmatism, and the Late Triassic A-type granites can provide new constraints for the tectonic evolution in this area. In this paper, we present a detailed investigation of zircon U-Pb dating, whole rock geochemistry and Hf isotopes of the Langmaitan syenogranite in the eastern segment of East Kunlun, in order to identify the chronology and petrogenesis of rocks, and provide a basis data for the evolution of regional tectonics. Syenogranite consists mainly of orthoclase, perthite, plagioclase, quartz, and a small amount of biotite. The zircon U-Pb dating yields an age of 231.5 ± 1.7 Ma, indicating its emplacement in Late Triassic. The syenogranite is geochemically characterized by high SiO_2 (72.36%~74.58%) and rich Al_2O_3 (12.76%~12.89%); is relatively rich in K_2O (7.52%~7.89%), but poor in Na_2O (4.0%~4.25%), low in MgO and TiO_2 ; enriched in large ion lithophilic elements Rb, K, etc., depleted in high field strength elements such as Ba, Nb, Ta, P, Ti, and displays significantly negative europium anomalies ($\delta\text{Eu}=0.04\sim0.08$). All these characteristics indicate that they are A-type granites. $\text{Mg}^\#$ is between 0.40 and 0.43, the $\epsilon_{\text{Hf}}(t)$ value is between +2.05 and +7.53, and T_{DM2} ages between 782 Ma and 1132 Ma, indicating that the syenogranite involvement of mantle components in petrogenesis. Based on the comprehensive regional geology and the characteristics, it is concluded that the Langmaitan A-type granite formed by partial melting of juvenile crust and mixed with mantle-derived materials in post-collision extensional environment.

Key words: syenogranite; zircon U-Pb dating; geochemistry; Lu-Hf isotopes; East Kunlun